

# Longitudinal Metabolite Changes after Traumatic Brain Injury: A Prospective Pediatric Magnetic Resonance Spectroscopic Imaging Study

Barbara Holshouser,<sup>1</sup> Jamie Pivonka-Jones,<sup>2</sup> Joy G. Nichols,<sup>2</sup> Udo Oyoyo,<sup>1</sup> Karen Tong,<sup>1</sup>  
Nirmalya Ghosh,<sup>2</sup> and Stephen Ashwal<sup>2</sup>

## Abstract

The aims of this study were to evaluate longitudinal metabolite changes in traumatic brain injury (TBI) subjects and determine whether early magnetic resonance spectroscopic imaging (MRSI) changes in discrete brain regions predict 1-year neuropsychological outcomes. Three-dimensional (3D) proton MRSI was performed in pediatric subjects with complicated mild (cMild), moderate, and severe injury, acutely (6–17 days) and 1-year post-injury along with neurological and cognitive testing. Longitudinal analysis found that in the cMild/Moderate group, all MRSI ratios from 12 regions returned to control levels at 1 year. In the severe group, only cortical gray matter regions fully recovered to control levels whereas N-acetylaspartate (NAA) ratios from the hemispheric white matter and subcortical regions remained statistically different from controls. A factor analysis reduced the data to two loading factors that significantly differentiated between TBI groups; one included acute regional NAA variables and another consisted of clinically observed variables (e.g., days in coma). Using scores calculated from the two loading factors in a logistic regression model, we found that the percent accuracy for classification of TBI groups was greatest for the dichotomized attention measure (93%), followed by Full Scale Intelligence Quotient at 91%, and the combined memory Z-score measure (90%). Using the acute basal ganglia NAA/creatine (Cr) ratio alone achieved a higher percent accuracy of 94.7% for the attention measure whereas the acute thalamic NAA/Cr ratio alone achieved a higher percent accuracy of 91.9% for the memory measure. These results support the conclusions that reduced NAA is an early indicator of tissue injury and that measurements from subcortical brain regions are more predictive of long-term cognitive outcome.

**Keywords:** factor analysis; magnetic resonance spectroscopy; outcomes; pediatric; traumatic brain injury

## Introduction

AFTER TRAUMATIC BRAIN INJURY (TBI), there is often a discrepancy between functional deficits and imaging findings. The milder the injury, the more difficult it is to radiologically detect injury and to answer the question, “Is ‘normal appearing brain’ normal?” TBI is often a diffuse multi-focal injury that can produce a cascade of cellular and metabolic alterations.<sup>1,2</sup> The location and severity of injury greatly affects the degree of metabolic and structural alterations; therefore, a technique that simultaneously can sample multiple brain regions is optimum for fully evaluating the heterogeneity, distribution, and severity of injury. Whether the injury is mild or severe, tools are needed to reliably predict patient outcomes and direct immediate clinical decision-making and long-term rehabilitation efforts. Advanced magnetic resonance (MR)

imaging (MRI) techniques are now being used to detect injury not observed with computed tomography (CT) or conventional MRI and predict long-term outcome. Using one of these techniques, proton MR spectroscopy (MRS), studies have demonstrated that changes in key brain metabolites, such as N-acetylaspartate (NAA), a measure of neuronal loss or dysfunction, and choline (Cho), a measure of membrane synthesis or disruption and inflammation, can detect brain injury that may be remote from TBI lesions and that appears normal on structural MRI.<sup>3–5</sup>

Although a number of studies have correlated single-voxel MRS findings with neuropsychological deficits in adults<sup>6–10</sup> and children,<sup>11–13</sup> only a few have used multi-voxel MR spectroscopic imaging (MRSI) to evaluate TBI in children and correlate these findings with neuropsychological outcomes. One two-dimensional (2D)/MRSI study through the supraventricular white matter showed

<sup>1</sup>Department of Radiology, Loma Linda University School of Medicine, Loma Linda, California.

<sup>2</sup>Department of Pediatrics, Loma Linda University School of Medicine, Loma Linda, California.

that elevated creatine (Cr; a marker of cell energy metabolism), was predictive of changes in executive function<sup>14</sup> whereas another study through the same area showed that a reduction of NAA/Cr and elevation of Cho/Cr in injured brain during the subacute phase predicted neuropsychological performance.<sup>15</sup> Our previous 2D-MRSI study through the level of the corpus callosum (CC) showed that reduced NAA/Cr measured within 16 days after injury in normal-appearing brain predicted long-term outcome more accurately than ratios arising from visibly injured brain.<sup>16</sup> A few longitudinal studies have been carried out in children. One 2D-MRSI study in children showed that elevated Cho and reduced NAA at 5 months post-injury in the splenium correlated with neurocognitive performance, and that NAA partially normalized whereas Cho fully normalized at a chronic (14.7 months) time point.<sup>17</sup>

Because TBI is often diffuse and multi-focal, techniques such as three-dimensional (3D)/MRSI and whole-brain MRSI have been developed to allow greater brain coverage. A recent longitudinal whole-brain MRSI study in moderate/severe pediatric TBI patients showed elevated Cho in all four brain lobes and the CC as well as decreased NAA in the CC at 3 months after injury in all patients.<sup>18</sup> Further, at 16 months after injury, low Cho and NAA were not significant predictors of cognition in a subgroup of patients with slow interhemispheric transfer time (IHTT), but chronically elevated Cho and NAA in the normal IHTT subgroup correlated with cognitive performance.<sup>18</sup> In another whole-brain study in adults, widespread elevation of Cho and Cho/NAA and a reduction of NAA and NAA/Cr with mild-to-moderate injury showed correlation of neuropsychological (NP) tests with frontal lobe Cho/NAA.<sup>19</sup> In a similar population, the same group found increased Cho throughout the cerebrum and cerebellum with highest levels in patients with the worst cognitive performance.<sup>20</sup>

In this study, we present our findings using 3D proton MRSI in pediatric patients with complicated mild, moderate, and severe injury, acutely (6–17 days) and at 1 year post-injury. The aims of our study were to evaluate longitudinal metabolite changes in TBI subjects and determine whether early MRS changes in discrete regions of the brain predict NP outcome 1 year after injury. Because of the large number of variables, we used factor analysis as a data reduction method to identify *in vivo* metabolite patterns in many regions after injury and their association with neurocognitive outcome.

## Methods

### Study population

This study was approved by our institutional review board. Written consent was obtained from all subjects' parents or legal guardian. In addition, consent was obtained from the subject if >11 years of age and assent was obtained from subjects between ages 7 and 11 years. TBI subjects were enrolled consecutively subsequent to hospital admission if consent was obtained and if they met the following criteria: 1) age between 4 and 18 years at the time of injury; 2) absence of previous brain injury, neurological disorders, drug or alcohol abuse, or MRI contraindications, including dental braces; 3) moderate-to-severe TBI with Glasgow Coma Scale (GCS) scores between 3 and 12 or complicated mild (cMild) TBI (GCS 13–15) if hemorrhage was detected on an acute brain imaging (CT) exam. Justification for including subjects with cMild TBI is based on the Mayo TBI Severity Classification System, which reclassifies subjects into the moderate-severe injury category in the presence of known brain injury such as intracerebral, subdural or epidural hematomas, subarachnoid hemorrhage, or contusion confirmed by radiological imaging.<sup>21</sup> Control subjects who met criteria 1 and 2 were recruited from our pediatric clinics and were

scanned without sedation. We took time to familiarize nonsedated children with the scanner environment to ensure that they were comfortable before scanning in order to decrease the failure rate. Images and spectra were checked for motion and repeated when necessary and as allowed by the subject.

### Data acquisition methods

TBI subjects were scanned acutely, within 6–17 days and at 1 year after injury. Controls were scanned twice, 1 year apart using the same protocol. Whole-brain MRI scans were acquired on a 3T whole-body imager (Trio/Tim; Siemens Medical Solutions, Erlangen, Germany) using a 12-channel receive-only head array coil. Imaging included an isotropic 3D sagittal T1-weighted inversion prepared fast spoiled gradient echo sequence (repetition time [TR]/echo time [TE]=1950/2.26 ms, number of excitations [NEX]=1, voxel size  $1.0 \times 1.0 \times 1.0 \text{ mm}^3$ ) and a 3D sagittal T2-weighted fast spin echo sequence with variable flip angles (TR/TE=3200/415 ms, NEX=1, voxel size  $1.0 \times 1.0 \times 1.0 \text{ mm}^3$ ). In addition, fluid-attenuated inversion recovery (FLAIR), susceptibility-weighted imaging and diffusion tensor-weighted images were acquired.

3D proton MRSI was acquired using a volume-selective, water-suppressed, point-resolved spectroscopy sequence (PRESS) with a TR=1700 msec, TE=144 msec, NEX=1, elliptical k-space weighting, 1024 data points sampled with a dwell time of 1 ms for an acquisition time of 17.1 min. Images from three orthogonal planes acquired during the imaging portion of the study were used for slab placement to match positioning along the anterior commissure-posterior commissure line. Manual shimming was performed to obtain signal line widths or a full width half maximum of <20 Hz and 3D-MRSI using phase encoding in the z-direction to obtain four or five 10-mm-thick slices, a  $160 \times 160 \times 80 \text{ mm}$  field-of-view, and  $16 \times 16 \times 8$  phase encoding arrays in the x-y-z direction for an individual voxel volume of 1 cc. The number of slices in the z direction and the volume of interest (VOI) size in the x-y directions within each slice varied and depended on the size of the brain. The slice thickness within the VOI was kept at 10 mm for all subjects. For example, in younger children, an  $8 \times 8$  VOI (64 voxels) in each of four 10-mm-thick slices for a total of 256 voxels (Fig. 1) was typically acquired compared to older children in which an  $8 \times 9$  VOI (72 voxels) in each of five 10-mm-thick slices for a total of 410 voxels was acquired. The slabs for each subject were positioned to cover from the level of the mid-CC through the superior brainstem (BS), including portions of the gray and white matter in the frontal (FG; FW), parietal (PG; PW), temporal (TG; TW), occipital gray matter (OG), cerebellum (CB), basal ganglia (BG), and thalami (TH). Saturation bands were used to suppress chemical shift artifacts arising from lipids outside the VOI. MRSI spectra were post-processed using LCModel (LCModel Version 6.0; Stephen Provencher Inc., Oakville, Ontario, Canada). For each MRSI voxel, individual metabolite concentrations were reported with a Cramer Rao estimation of the lower bounds of measurement error, CRLB percentage (CRLB%), reflecting maximum-likelihood estimates and their uncertainties. Peak concentrations for NAA (2.02 ppm), total Cr (3.02 ppm), total Cho (3.20 ppm), and lactate (Lac), if present (identified as an inverted doublet at 1.33 ppm and 7-Hz splitting), were measured and recorded for each individual MRSI voxel in a spreadsheet for further analysis. Metabolite ratios were then calculated (NAA/Cr, NAA/Cho, Cho/Cr, and Lac/Cr) for each voxel. Brain segmentation and 3D registration techniques were used to calculate the percentage of gray, white, and cerebrospinal fluid in each voxel and make region assignments as described previously.<sup>22</sup> For statistical analyses, the following limiting criteria were applied to ensure that the data chosen were based on quality spectra. As a start, metabolite concentrations with a CRLB% of 20 or less for TBI and 10% or less for control subjects for at least one of the three main metabolites (NAA, Cr, or Cho) were included. This resulted in the inclusion of approximately 90%

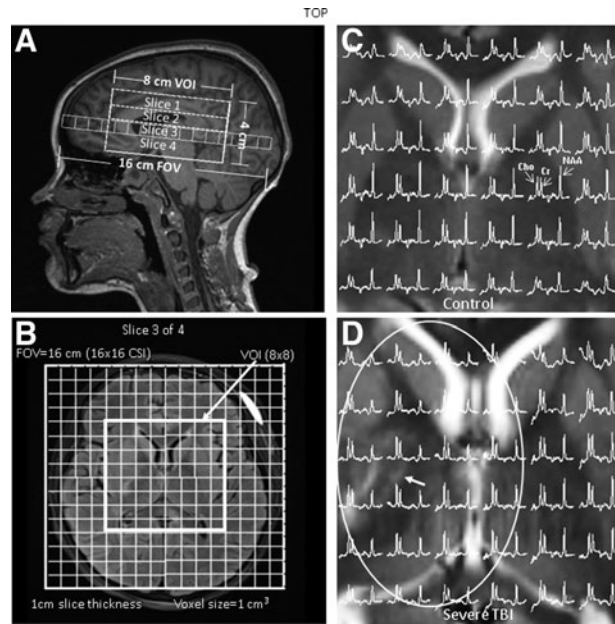


**FIG. 1.** Positioning of the 3D-MRSI VOI on (A) sagittal T1-weighted and (B) axial T2-weighted FLAIR MRI illustrating a  $16 \times 16 \times 4 \text{ cm}^3$  FOV and  $8 \times 8 \times 4 \text{ cm}^3$  VOI. Phase encoding along the z-axis was used to acquire four 10-mm-thick slices. The FOV size, voxel size ( $1 \text{ cm}^3$ ), and slice thickness remained the same for all subjects. The VOI in the x-y direction and number of slices in the z direction varied by age to accommodate brain size. (C)  $^1\text{H}$  spectra from the central portion of the VOI on a T2-weighted axial image at the level of the basal ganglia from a 10-year-old female control subject showing normal levels of NAA, Cr, and Choline. (D)  $^1\text{H}$  spectra from the central portion of the VOI on a T2-weighted axial image at the level of the basal ganglia from a 10-year-old female TBI subject involved in a motor vehicle accident (GCS 3) with an area of T2 lengthening (arrow) in the right basal ganglia/thalamus.  $^1\text{H}$  spectra within the ellipsoid show decreased NAA levels compared to the contralateral side and the control subject. Note: sagittal (A) and axial (B) images are from the same TBI subject. 3D, three-dimensional; Cr, creatine; FOV, field of view; GCS, Glasgow Coma Scale; MRSI, magnetic resonance spectroscopic imaging; NAA, N-acetylaspartate; TBI, traumatic brain injury; VOI, volume of interest.

of spectra for most subjects. Of particular concern was to avoid excluding too much data from TBI subjects with injury resulting in low metabolite levels, thus higher CRLB% and lower signal-to-noise ratio. Therefore, all spectra were visually inspected and excluded only if they showed excessive distortion, artifacts, and/or lipid contamination. For example, spectra near hemorrhagic lesions in TBI subjects tended to have major distortion artifacts or were missing peaks and could not be included. In addition, CB, BS, and OG measurements were prone to spectral distortions attributed to location; therefore, these data are missing in 29% of our control subjects and in up to 50% of our TBI subjects. Next, a fractional tissue volume criterion was applied to only include voxels with underlying tissue volume of 80% or more. Finally, an outlier exclusion criterion was applied to exclude voxels with metabolite values greater than 3 times the standard deviation (SD) of the corresponding metabolite value over all the voxels within a particular region which excluded approximately 1% or less of voxels. For each subject, data from included voxels were then used to calculate mean metabolite ratios for each region.

NP assessments were conducted at 3 months and 1 year after injury for TBI subjects and twice, 1 year apart, for controls at the

outpatient LLU Pediatric NeuroAssessment Program (PNAP clinic). Only the 1-year NP testing results were used in this report. The NP battery included measures of general intelligence (Wechsler Abbreviated Scales of Intelligence [6–18 years] or Wechsler Preschool Primary Scale of Intelligence [4–5 years]), attention (Sky Search subtest from the Test of Everyday Attention for Children (TEA-Ch-G; 6–16 years)), and memory (Children's Memory Scale [5–17 years] or Wechsler Memory Scale [17–18 years]). The Full Scale Intelligence Quotient (FSIQ) was used as an NP outcome. Memory scores were converted to z-scores for ease of statistical comparison across measures.

A Pediatric Cerebral Performance Category Scale score (PCPCS) was assigned by a pediatric neurologist to assess neurological outcome. Serial neurological examinations were performed in TBI patients at six time points (study entry, acute MRI, hospital discharge, and 3, 6, and 12 months) and twice for controls, 1 year apart. Clinical data collected during hospital stay on TBI subjects were also recorded in the database.

### Statistical analysis

Subjects were grouped as controls, cMild/Moderate TBI (GCS = 9–15), or Severe TBI (GCS = 3–8). This grouping was used in an analysis of covariance (ANCOVA) to test for significant group differences for metabolite ratios and 1-year NP testing scores using age as a covariate. Bonferroni post-hoc tests were used as appropriate to control for multiple comparisons. Paired *t*-tests were used to test for significant longitudinal metabolite ratio changes within each group at an alpha level of 0.001 to adjust for multiple comparisons. Spearman correlations were calculated to determine associations between MRSI metabolite ratios, clinical variables, and neurological and NP outcomes. All statistical analyses were performed in SPSS software (version 22; SPSS, Inc., Chicago, IL).

Factor analysis, a method previously used by Mohamed and colleagues,<sup>23</sup> was performed using the principal components of 27 MRSI variables and five clinically observed variables to generate eigenvectors. Ratios from the BS, CB, and OG regions were omitted because of data sparsity. Only eigenvectors with eigenvalues greater than 1 were kept. Varimax rotation with Kaiser normalization was applied to produce five factors that explained 81.5% of the variance. Only strong factor loadings over 0.6 were accepted. Each subject was assigned a score for each of the five rotated factors on the basis of the loadings. *t*-tests determined that two of the five scores could differentiate cMild/Moderate TBI versus Severe TBI.

Scores that differed significantly between TBI groups were subsequently used in a binary logistic regression to predict 1-year neurological and NP outcomes. To do this, the 1-year NP outcomes (memory Z-score, attention, and FSIQ) were dichotomized by utilizing a cutoff at 1.50 SDs below the normative mean, which yielded the following groupings: scores above the cutoff (scaled scores  $>5$  and standard scores  $>78$ ;  $>-1.50$  SDs) comprised Group 1 (Not Impaired) and scores below the cutoff (scaled scores  $<6$  and  $<79$ ;  $<-1.49$  SDs) comprised Group 2 (Impaired). The PCPCS was dichotomized into Not Impaired (PCPCS = 1–3) or Impaired (PCPCS = 4–6). Each dichotomized NP outcome (memory, attention, and FSIQ) or dichotomized PCPCS was separately input as the dependent variable in a binary logistic regression to determine how well the independent variables (i.e., scores from the factor analysis or individual MRS parameters such as BG NAA/Cr) could accurately predict whether the patient was impaired or not impaired.

## Results

### Clinical demographics

Data reported in this study are from a total of 64 TBI and 63 control subjects who were enrolled in the study and completed

follow-up imaging and NP assessments. Table 1 compares the distribution of age, sex, timing of MRI exams, GCS score, type of accident, significant clinical data for each TBI group, and 12-month outcomes for all study groups. There were significantly more males in the TBI groups compared to controls ( $p=0.002$ ). In the cMild/Moderate TBI group, 25 of 32 were assigned an admission GCS between 13 and 15, but qualified for the study after findings of hemorrhage or hematoma were detected on their admission CT exam. Their admission GCS scores were used for calculations in Table 1. In addition to the subjects enrolled in the study, a total of 32 TBI and 18 control subjects did not complete testing for the following reasons; 5 TBI and 7 control subjects dropped out of the study before MRI occurred, 16 TBI and 3 control subjects moved out of the area or refused to return for follow-up, 7 TBI and 4 control subjects refused to continue during the first MRI, 2 control subjects were dropped after NP assessments, and 4 TBI and 2 control subjects refused to return for the final NP assessment.

Severely injured TBI subjects were in coma, on a ventilator, and in the hospital significantly longer than subjects in the cMild/Moderate group (Table 1). Loss of consciousness (LOC), categorized into three groups (no LOC, LOC <24 h, and LOC >24 h), was also significantly different between groups with all subjects in the severe group experiencing LOC. Neurological outcome measured as mean PCPCS score at 12 months was significantly higher in the severe group, with 19 subjects categorized as normal, 8 subjects with mild disabilities, 4 subjects with moderate disabilities, 1 subject with severe disabilities, and no subjects in a vegetative state or who died. In the cMild/Moderate group, most subjects recovered to normal PCPCS at 12 months with only 1 subject categorized as

having mild deficits. Measures of NP outcome at 12 months varied from no significant differences between groups in terms of FSIQ to significant differences between groups on measures of attention (TEA-Ch-G) and memory (combined memory Z-score;  $p=0.003$  and  $p=0.001$ , respectively; Table 1).

#### Analysis of longitudinal magnetic resonance spectroscopic imaging factors

Regional MRSI ratios between study groups for the acute and 12-month (12-Mo) time points with results of statistical analysis are listed in Supplementary Table 1. (see online supplementary material at <http://www.liebertpub.com>) Longitudinal MRSI data for the controls were compared using paired *t*-tests at an alpha level of 0.001 to adjust for multiple comparisons. No statistically significant differences in MRS ratios for controls between the two time points were observed, indicating no significant age-related metabolite changes. Although several regional comparisons reached lower levels of significance (0.03–0.05) in controls, the actual differences were not considered clinically significant (difference >2 SDs). Metabolite recovery, as indicated by increases in NAA ratios and decreases in Cho/Cr ratios, was observed in all regions in both TBI groups, some of which were significant at  $p \leq 0.001$  (Supplementary Table 1). (see online supplementary material at <http://www.liebertpub.com>) Using an ANCOVA to evaluate differences between groups at each time point, we found that in the cMild/Moderate group, all MRSI ratios returned to control levels even in regions such as the BG, TH, FG, and OG in which the NAA/Cr ratios were reduced at the acute time point ( $p \leq 0.001$ ). In

TABLE 1. DEMOGRAPHICS, NEUROLOGICAL, AND COGNITIVE ASSESSMENT SCORES FOR GROUPS

	Control group (n = 63)	cMild/moderate TBI (n = 32)	Severe TBI (n = 32)	P value*
Age at initial study (years)	12.6 ± 3.3	12.2 ± 3.3	12.0 ± 3.8	0.65
Range, median (years)	5.5–17.4, 13.3	4.4–17.2, 13.3	4.9–18.0, 12.6	
Sex	33 M/30 F	26 M/6 F	21 M/11 F	0.014
Time to MRI after injury (days)	NA	11.7 ± 3.2	11.5 ± 3.7	0.774
Range, median (days)		6–17, 12.0	6–20, 10.7	
Time to follow-up MRI (months)	12.7 ± 1.1	12.2 ± 0.96	12.1 ± 0.63	0.002
Range, median (months)	11.0–16.7, 12.6	10.7–14.5, 11.9	10.8–13.3, 12.1	
Average GCS score	NA	13.6 ± 2.0	4.4 ± 1.8	NA
Median		14	4	
Accident type	NA	11 falls, 6 MVA, 6 hit by MV, 6 sports, 2 ATV, 1 fight	3 falls, 10 MVA, 15 hit by MV, 3 ATV, 1 boating	
Days in coma	NA	0.63 ± 0.55	5.53 ± 5.81	<0.001
Days on ventilator	NA	0.03 ± 0.18	5.47 ± 4.54	<0.001
Days in hospital	NA	5.88 ± 3.01	17.4 ± 10.1	<0.001
Seizures (epilepsy)	NA	4	8 (2)	0.081
Loss of consciousness (none, <24 h, >24 h)	NA	(12, 19, 1)	(0, 13, 19)	<0.001
PCPCS @ 12 months	1.0 ± 0.0	1.03 ± 0.18	1.59 ± 0.84	<0.001
Test of Everyday Attention – TEA-Ch-G @ 12 months	10.88 ± 3.4 (n = 48)	11.86 ± 3.09 (n = 29)	9.04 ± 3.81 (n = 28)	<0.001
Combined Memory Z Score @ 12 months	1.14 ± 1.03	0.829 ± 1.080	–0.3796 ± 1.5900	<0.001
FSIQ @ 12 months	108.0 ± 14.6	96.56 ± 13.90	92.03 ± 13.10	0.230

Values denote means ± standard deviation.

\**p* values for sex, presence of seizures, and loss of consciousness represent Pearson  $\chi^2$  test; all others represent non-parametric Kruskal-Wallis or analysis of covariance between-groups significance.

MRI, magnetic resonance imaging; GCS, Glasgow Coma Scale; PCPCS, Pediatric Cerebral Performance Category Scale score; TEA-Ch-G, Test of Everyday Attention for Children; FSIQ, Full Scale IQ; TBI, traumatic brain injury; cMild, complicated mild; ATV, all-terrain vehicle; MVA, motor vehicle accident; MV, motor vehicle; ED, emergency department; NA, not applicable.

the severe group, all cortical gray matter regions (except TG) fully recovered to control levels at 12 months whereas other regions remained statistically different from controls (Supplementary Table 1). (see online supplementary material at <http://www.liebertpub.com>) NAA/Cr and NAA/Cho ratios were significantly reduced in multiple regions at 12 months (Fig. 2, Supplementary Table 1). Figure 3A and 3B plot longitudinal recovery of NAA/Cr ratios from the BG and TH in TBI groups compared to controls. Similar plots for NAA/Cho ratios are presented in supplementary material (Supplementary Fig. 1) (see online supplementary material at <http://www.liebertpub.com>). Also, in the severe group, the Cho/Cr ratio was significantly elevated acutely in the TG and TW; however, at 1 year, the BG, CC, FW, PW, and TG regions showed significant Cho/Cr elevations (Supplementary Table 1). (see online supplementary material at <http://www.liebertpub.com>)

#### Metabolite ratios and correlation with clinical variables and outcomes

Strong significant ( $p \leq 0.001$ ) correlations (Spearman;  $-0.5$  to  $-0.8$ ) were observed between early NAA ratios (from the BG, BS, CC, PG, PW, TG, TW, and TH regions) and clinical variables (days in coma, days on ventilator, days in hospital, and LOC), but not the presence of seizures. Correlations between early regional Cho/Cr ratios and clinical variables were weak and nonsignificant. Early NAA ratios from the BG, BS, CC, FG, FW, PG, PW, TG, TW, and TH showed strong significant ( $p \leq 0.001$ ) correlations (Spearman;  $-0.5$  to  $-0.8$ ) with the PCPCS score assessed at 12 months. None of the early regional Cho/Cr ratios correlated with 12-month PCPCS scores.

A few of the early regional NAA/Cr ratios showed strong correlations with 12-month NP memory and attention, but not FSIQ. For the composite memory Z score, we saw strong associations ( $0.5$ – $0.6$ ) with the BS and CC ( $p \leq 0.001$ ), and for the attention

measure, we observed strong associations with the BG, TW, and TH ( $p \leq 0.001$ ). None of the early regional Cho/Cr ratios correlated with the cognitive assessments.

#### Factor analysis of acute magnetic resonance spectroscopic imaging regional and clinical variables to predict outcome

Factor analysis was utilized to determine associations between metabolite ratios across regions and other clinically observed data. The associations or factor loadings and percentage of variance explained are listed in Supplementary Table 2. (see online supplementary material at <http://www.liebertpub.com>) Scores for each factor were calculated for each patient and tested to determine whether the scores could distinguish between TBI groups (cMild/Moderate vs. Severe). Testing showed that two factors were significant ( $t$ -test;  $p < 0.001$ ). Factor 1, "NAA factor" (Supplementary Table 2), (see online supplementary material at <http://www.liebertpub.com>) showed major contributions from one or both NAA metabolite ratios from seven regions (BG, CC, FG, FW, PW, TW, and TH). Factor 3, "Clinical factor," showed major contributions from four of the five clinically observed variables included (days in coma, days on ventilator, days in hospital, and LOC). Factor 2, "Cho factor," showed major contributions from Cho/Cr ratios from nine regions, but could not distinguish between TBI groups when tested ( $p = 0.693$ ). Factors 4 and 5 showed few contributions and could not distinguish between TBI groups. Scores for factors 1 (NAA factor) and 3 (clinical factor) were used as independent variables in a binary logistic regression analysis to predict either dichotomized memory, FSIQ, or attention outcomes (dependent variables).

Using both the NAA and clinical factor scores as covariates in the logistic regression, the percent accuracy for classification was

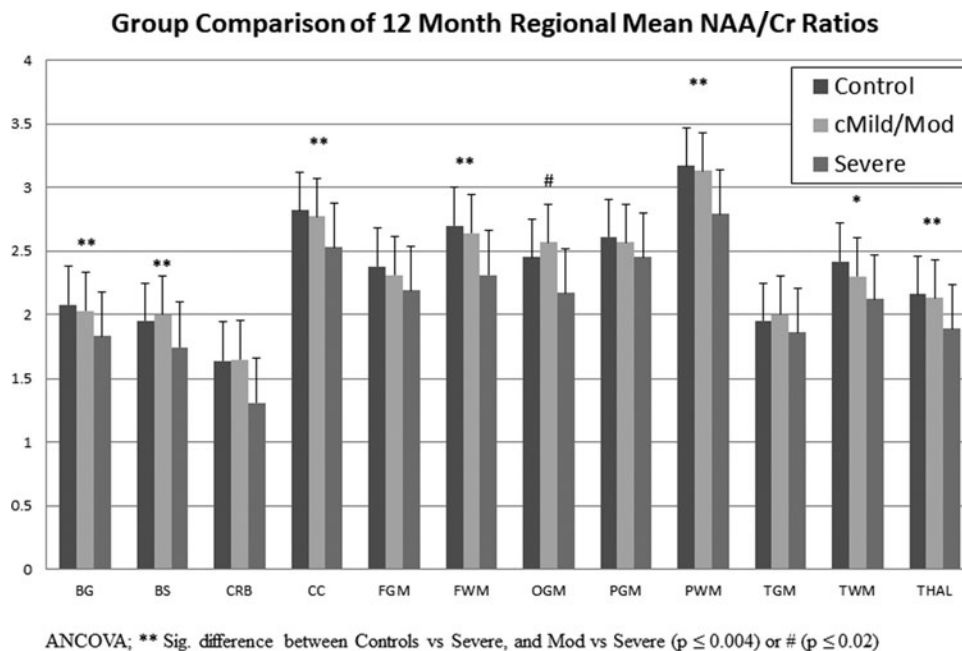


**FIG. 2.** A plot of the mean NAA/Cr ratios for each region measured at 12 months after injury in TBI groups compared to age-matched control values. ANCOVA was used corrected for age. \*\*Indicates a significant difference between Controls versus Severe and Mod versus Severe ( $p \leq 0.004$ ) or # ( $p \leq 0.02$ ). \*Indicates a significant difference between Controls versus Severe ( $p = 0.001$ ). ANCOVA, analysis of covariance; cMild, complicated mild; Cr, creatine; NAA, N-acetylaspartate; TBI, traumatic brain injury.

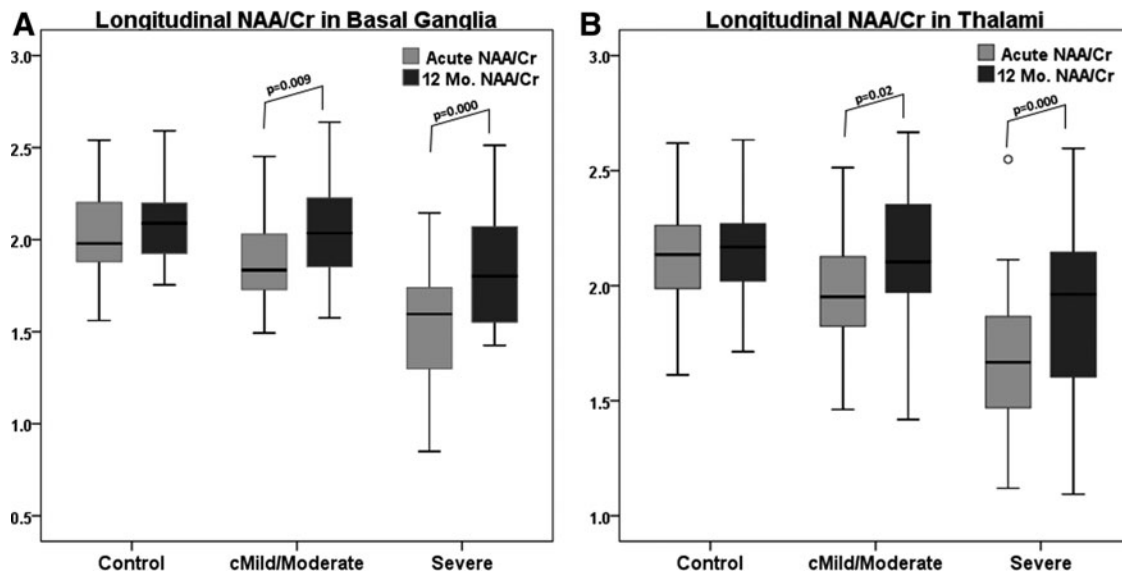


**FIG. 3.** Box plots displaying mean NAA/Cr ratios, 95% confidence intervals (whiskers), and outliers (°) from the (A) basal ganglia and (B) thalami for control subjects measured at enrollment and at 1 year and for TBI groups measured acutely (6–17 days) and 12 months after injury. cMild, complicated mild; Cr, creatine; NAA, N-acetylaspartate; TBI, traumatic brain injury.

greatest for the dichotomized attention measure, Tea-Ch-G (93%), followed by FSIQ (90.6%), combined memory Z-score measure (90.3%), and PCPCS (87.5%; Table 2). Acute NAA/Cr ratios from two regions, BG and TH, showed the highest loading factors and highest correlations with outcome measures and were input individually as covariates into the logistic regression to compare predictive accuracy with the factors model. Thalamic NAA/Cr ratios achieved a higher percent accuracy for classification and accounted for a higher percentage of the variance for the memory Z-score and the FSIQ measures compared to the factors model or BG NAA/Cr. BG NAA/Cr ratios achieved a higher percent accuracy for classification for the PCPCS outcome score and the attention measure than the factors model or TH NAA/Cr. In addition, the TH NAA/Cr

ratio combined with the days in hospital clinical factor achieved the highest overall accuracy of 93.8% for FSIQ, and the BG NAA/Cr ratio combined with days in hospital achieved the highest overall accuracy of 90.6% for PCPCS with the highest sensitivity (71.4%), and accounted for the most variance. In general, specificities in the range of 96–100% were achieved compared to sensitivities in the range of 16–71%, indicating better ability to predict recovery rather than impairments with these models.

**Discussion**

The key findings of the current study are that early NAA metabolite reductions in several subcortical regions are primary

**TABLE 2. RESULTS OF BINARY LOGISTIC REGRESSION TO PREDICT 12-MONTH NEUROLOGICAL AND NEUROPSYCHOLOGICAL OUTCOMES**

12-month dichotomized outcomes	% Sensitivity	% Specificity	Overall % accuracy	p value for model	% variance explained <sup>a</sup>
<b>Combined Memory Z Score</b>					
Factors 1 + 3	44.4	98.1	90.3	0.003	30.6
BG NAA/Cr	33	100	90.3	0.001	28.1
TH NAA/Cr	44.4	100	91.9	0.000	32.2
<b>TEA-Ch-G Attention Measure</b>					
Factors 1 + 3	40	98.1	93	0.010	33.3
BG NAA/Cr	40	100	94.7	0.007	26.8
TH NAA/Cr	40	98.1	93	0.000	42.9
<b>Full Scale IQ</b>					
Factors 1 + 3	0	100	90.6	0.049	19.4
BG NAA/Cr	0	100	90.6	0.022	16.9
TH NAA/Cr	16.7	100	92.2	0.003	27.7
TH NAA/CR + Days in Hosp	33.3	100	93.8	0.009	29.2
<b>PCPCS</b>					
Factors 1 + 3	50	98	87.5	0.000	46.1
BG NAA/Cr	50	98	87.5	0.000	33.2
TH NAA/Cr	35.7	96	82.8	0.000	31.4
BG NAA/CR + Days In Hosp	71.4	96	90.6	0.000	47.6

<sup>a</sup>Estimated with Nagelberke R square; factor 1 represents acute NAA ratios from seven regions; factor 3 represents clinically observed variables (days in coma, days on ventilator, days in hospital, loss of consciousness). All metabolite ratios were measured at the acute time point.

BG, basal ganglia; PCPCS, Pediatric Cerebral Performance Category Scale score; Tea-Ch-G, Test of Everyday Attention for Children; TH, thalamus.

factors that are associated with long-term neurological and NP outcomes. We found that all metabolite ratios recovered to control levels in cMild/Moderate TBI patients in all regions at 1 year, whereas NAA ratios in TBI patients with severe injury recovered to control levels only in the cortical gray matter (Fig. 2). Further, in severely injured subjects, NAA ratios in subcortical gray (BG, TH) and white matter (CC) regions remained significantly reduced compared to controls, yet recovered to a greater extent than NAA ratios in hemispheric WM regions (FW, PW, and TW). Cho/Cr ratios changes were less extensive than changes in NAA ratios in the severe TBI group, with only two regions (TG, TW) showing significant elevations at the acute time point, which did not correlate with long-term cognitive outcomes. At 1 year, however, multiple regions (BG, CC, FW, PW, and TG) were significantly elevated (Supplementary Table 1). (see online supplementary material at <http://www.liebertpub.com>) This may be in response to long-term neuroinflammation or an indication of recovery with cellular proliferation.<sup>5,24</sup>

It is hypothesized that early reductions in NAA ratios reflect changes in neuronal and axonal density. At the time of measurement, it is unknown whether these early NAA reductions represent dysfunction attributed to reduced or altered mitochondrial activity in which cells may recover, or whether these reductions represent irreversible neuronal loss that will lead to long-term deficits.<sup>4,25,26</sup> Studies of pediatric TBI models have demonstrated that the ability of alternative substrates to rescue brain metabolism may be developmentally regulated, that metabolic derangements begin early and are sustained after TBI, that neuronal oxidative metabolism of glucose is delayed, and that mitochondria have significant alterations in respiratory capacity, all of which can affect metabolic recovery and NAA levels.<sup>25</sup> In one MRS study, mitochondrial impairment, measured as percent NAA/Cr reduction, decreased soon after injury and reached a nadir at 10 days. Subsequently, NAA/Cr recovered in patients with favorable outcome, but remained impaired in patients with poor outcome.<sup>26</sup> In the current study, subjects with milder injury showed smaller reductions of acute NAA ratios. In fact, most regions were not significantly different from control values, and, as expected, all subjects except 1 recovered to normal neurological outcomes. As suggested in earlier studies, it is possible that there is a threshold of injury below which cells cannot recover,<sup>27</sup> and that NAA measurements have prognostic value to assist in management and to serve as a surrogate endpoint for clinical trials.<sup>26</sup>

An issue is which region(s) should be sampled to yield the most sensitive and specific data to best determine prognosis (given the variability in injury severity and trajectory of neuronal degeneration/recovery for each region) given that recovery from certain regions may better correlate with specific neurocognitive outcomes. In a previous study, we showed that sampling normal-appearing brain more accurately predicts prognoses than sampling areas with evident injury.<sup>16</sup> In the current study, we show that early reductions of NAA ratios, particularly from subcortical gray matter regions, were most predictive of neurological and cognitive recovery. It is interesting that the NAA ratios from subcortical gray matter regions correlated more strongly with neurological and neurocognitive outcomes and were stronger contributors in the factor analysis model than hemispheric white matter ratios. In fact, the NAA/Cr ratios from the TH alone showed a higher percent accuracy in classifying both general intellectual and memory functions than the factor analysis model that included ratios from nine regions (Table 2). Moreover, BG NAA/Cr alone showed higher percent accuracy in classifying neurological outcome and

recovery of focused attention 1 year post-injury than the factor analysis model. These findings agree with our previous work reporting that NAA measurements as well as lesion number and volume from susceptibility-weighted imaging (SWI) in deep brain regions, such as the BG, TH, and BS, were strongly associated (with large effect sizes observed) with almost all domains of intellectual and NP functioning.<sup>17</sup> This suggests that localization of specific neurocognitive functions is likely mediated by subcortical pathology, given that this region appears to serve as a primary gateway, or relay station, for the majority of higher cortical functions. The CC has consistently been correlated to severe TBI and NP outcome because callosal fibers reflect deep pathways across many functional modalities.<sup>28,29</sup> Others have associated injury to deep brain structures with long-term deficits in children. In 1974, Ommaya and Gennarelli<sup>30</sup> published their translational research related to the centripetal forces associated with TBI that was instrumental in developing the "depth of lesion model." A neuropathological scoring system originally reported by Adams<sup>31</sup> was used by Grados and colleagues in a cohort of 106 children (ages 4–19 years) with moderate-to-severe TBI in whom MRI was acquired and found that the depth of lesion classification significantly correlated with functional outcomes.<sup>32</sup> More recently, a meta-analysis of pediatric TBI studies reinforced that depth and severity of injury was highly predictive of neurocognitive outcome.<sup>33</sup>

Whereas focused attention is a functional domain known to be sensitive to TBI,<sup>33–35</sup> the organization of functional neural networks underlying this construct has been the subject of debate for more than half a century. Early work by Beck and colleagues<sup>36</sup> linked impairment in attention or alertness to frontal lobes systems; however, Penfield and Jasper's studies<sup>37</sup> of patients with absence seizures linked attention dysfunction to networks deep within the center of the brain (centrencephalic), which has been supported by recent functional imaging studies that appear to implicate the ascending brainstem reticular activating system as the neuroanatomical substrate of attention and arousal. The current findings, which link subcortical pathology with attention dysfunction and LOC, are not surprising and may overlap diagnostically with altered levels of alertness and disorders of consciousness.

In terms of memory, the measures included in the current study assessed declarative (explicit) memory (facts or events that can be consciously recalled). Previous work has suggested both a hippocampal-anterior thalamic axis and perirhinal-medial dorsal thalamic nuclei axis,<sup>38</sup> as well as a medial prefrontal-thalamic-hippocampal network, as contributing to encoding and recall of declarative memories, which may help explain why reductions in thalamic NAA were more prognostic of memory impairment than a factor model with ratios from seven regions.

Damage inflicted by TBI, as well as the potential outcome, depends not only on the local effects of the primary insult, but also on the secondary, delayed, nonmechanical processes consequent to axonal damage and Wallerian degeneration.<sup>39</sup> The subcortical nuclei of the basal ganglia are interconnected with the cerebral cortex, TH, BS, and several other brain regions. The thalamus is highly connected to white matter axons through thalamocortical pathways and is often described as the central relay station of the brain because it has reciprocal projections to the entire cerebral cortex and plays a principal role in the processing and transmission of information between sensory, motor, and associative regions.<sup>40</sup> Some have suggested that the thalami may be particularly vulnerable to secondary injury because of their interconnectiveness with white matter projections that are highly susceptible to injury during TBI,<sup>41–43</sup> resulting in volume loss<sup>41,44</sup> and disorders of consciousness.<sup>45,46</sup>

Recent functional MRI and positron emission tomography studies are defining the various networks that modulate cognitive states, and accumulating evidence indicates that communications between these networks are adversely affected after TBI. The most commonly identified networks that contribute to cognitive and motor impairments include the default mode, executive control, salience, and frontal mesocircuit networks, all of which have extensive connections to multiple cortical, subcortical, and brain stem regions.<sup>47–50</sup> As noted above, secondary nonmechanical degenerative processes triggered by brain injury continue weeks to months after injury and may target the associated networks and pathways, resulting in not only volume loss and functional MRI abnormalities, but also the metabolic changes observed in our study. We sampled metabolic recovery at 1 year after injury and found that the subcortical gray matter and CC regions were recovering, but had not returned to control levels, in severely injured subjects whereas the hemispheric WM regions showed little recovery. It is possible that the subcortical gray matter regions by way of striatal and corticothalamic pathways are particularly vulnerable to pathological and metabolic changes attributed to transneuronal cells, the extent of which becomes evident early after injury, making these regions particularly useful for long-term outcome prediction.

Limitations of the MRS methods used in this study include the use of metabolite ratios rather than quantitative measurements of metabolite levels. The use of Cr in ratios adds uncertainties, given that alterations of Cr have been reported in some brain injury studies,<sup>14,51</sup> but not others.<sup>19,52</sup> This may have masked changes in Cho, reported as Cho/Cr ratios, which were smaller in magnitude than NAA changes, given that we and others using varying techniques have previously shown significant elevations in Cho early after TBI.<sup>16,19</sup> After visual inspection of the spectra, we are confident that detected reductions of NAA ratios were attributed primarily to NAA reductions, rather than elevated Cr or Cho levels. Also, metabolite and water relaxation times (T1 and T2) were not accounted for, and therefore the reported MRSI measures include possible contributions from altered relaxation times. This reflects the practical difficulty of including the lengthy relaxation time measurement in the study protocol. Although the volumetric MRSI method used in this study sampled a much greater fraction of the brain volume (25–30%) than single-voxel studies, the method still leaves the majority of the brain volume unsampled, notably in frontotemporal regions, which may reflect important executive functions. We also encountered technical issues in brainstem and cerebellar regions and could not report complete data from those regions. Finally, for statistical purposes, the NP outcome data were transformed from continuous to dichotomized variables that likely removed some important variability and predictive power across the sample.

Our results support the conclusions that altered metabolism is an early indicator of tissue injury and that early NAA measurements from deeper brain regions, which reveal cellular dysfunction, are more predictive of long-term neurological and cognitive outcome. The longitudinal metabolite changes reported in this study show little metabolic recovery in hemispheric white matter regions after severe injury. This may indicate an ongoing functional or structural disconnect of functional networks between hemispheric white matter and subcortical regions, resulting in the cognitive deficits observed in our severely injured subjects. A multi-parametric approach, that includes diffusion tensor imaging (DTI) to provide information about the integrity of white matter pathways after TBI, would be useful. Additional data collected from this cohort using other imaging techniques such as SWI and DTI will be discussed in additional publications.

## Acknowledgments

The authors acknowledge and thank their MR technologists and pediatric nurse managers whose diligent work made this project possible. This work was supported by the National Institutes of Health (NIH; NINDS 5R01NS05400). The content is solely the responsibility of the authors and does not necessarily represent the official views of the NINDS or the NIH.

## Author Disclosure Statement

No competing financial interests exist.

## References

- Farkas, O., and Povlishock, J.T. (2007). Cellular and subcellular change evoked by diffuse traumatic brain injury: a complex web of change extending far beyond focal damage. *Prog. Brain Res.* 161, 43–59.
- Dennis, E.L., Babikian, T., Giza, C.C., Thompson, P.M., and Asarnow, R.F. (2018). Neuroimaging of the injured pediatric brain: methods and new lessons. *Neuroscientist* Feb 1. doi: 10.1177/1073858418759489. [Epub ahead of print].
- Astrakas LG, Argyropoulou MI. (2016). Key concepts in MR spectroscopy and practical approaches to gaining biochemical information in children. *Pediatr. Radiol.* 46, 941–951.
- Croall, I., Smith, F.E., and Blamire, A.M. (2015). Magnetic resonance spectroscopy for traumatic brain injury. *Top. Magn. Reson. Imaging* 24, 267–274.
- Chang L, Munsaka SM, Kraft-Terry S, and Ernst T. (2013). Magnetic resonance spectroscopy to assess neuroinflammation and neuropathic pain. *J. Neuroimmune Pharmacol.* 8, 576–593.
- Ariza, M., Junque, C., Mataro, M., Poca, M.A., Bargallo, N., Olondo, M., and Sahuquillo, J. (2004). Neuropsychological correlates of basal ganglia and medial temporal lobe NAA/Cho reductions in traumatic brain injury. *Arch. Neurol.* 61, 541–544.
- Brooks, W.M., Stidley, C.A., Petropoulos, H., Jung, R.E., Weers, D.C., Friedman, S.D., Barlow, M.A., Sibbitt, W.L., Jr., and Yeo, R.A. (2000). Metabolic and cognitive response to human traumatic brain injury: a quantitative proton magnetic resonance study. *J. Neurotrauma* 17, 629–640.
- Friedman, S.D., Brooks, W.M., Jung, R.E., Hart, B.L., and Yeo, R.A. (1998). Proton MR spectroscopic findings correspond to neuropsychological function in traumatic brain injury. *AJNR Am. J. Neuroradiol.* 19, 1879–1885.
- Shutter, L., Tong, K.A., Lee, A., and Holshouser, B.A. (2006). Prognostic role of proton magnetic resonance spectroscopy in acute traumatic brain injury. *J. Head Trauma Rehabil.* 21, 334–349.
- Sivak, S., Bittsansky, M., Grossmann, J., Nosal, V., Kantorova, E., Sivakova, J., Demkova, A., Hnilicova, P., Dobrota, D., and Kurca, E. (2014). Clinical correlations of proton magnetic resonance spectroscopy findings in acute phase after mild traumatic brain injury. *Brain Inj.* 28, 341–346.
- Ashwal, S., Holshouser, B.A., Shu, S.K., Simmons, P.L., Perkin, R.M., Tomasi, L.G., Knierim, D.S., Sheridan, C., Craig, K., Andrews, G.H., and Hinshaw, D.B. (2000). Predictive value of proton magnetic resonance spectroscopy in pediatric closed head injury. *Pediatr. Neurol.* 23, 114–125.
- Holshouser, B.A., Ashwal, S., Shu, S., and Hinshaw, D.B., Jr. (2000). Proton MR spectroscopy in children with acute brain injury: comparison of short and long echo time acquisitions. *J. Magn. Reson. Imaging* 11, 9–19.
- Brenner, T., Freier, M.C., Holshouser, B.A., Burley, T., and Ashwal, S. (2003). Predicting neuropsychologic outcome after traumatic brain injury in children. *Pediatr. Neurol.* 28, 104–114.
- Gasparovic, C., Yeo, R., Mannell, M., Ling, J., Elgie, R., Phillips, J., Doezema, D., and Mayer, A.R. (2009). Neurometabolite concentrations in gray and white matter in mild traumatic brain injury: an 1H-magnetic resonance spectroscopy study. *J. Neurotrauma* 26, 1635–1643.
- Yeo, R.A., Phillips, J.P., Jung, R.E., Brown, A.J., Campbell, R.C., and Brooks, W.M. (2006). Magnetic resonance spectroscopy detects brain injury and predicts cognitive functioning in children with brain injuries. *J. Neurotrauma* 23, 1427–1435.



16. Holshouser, B.A., Tong, K.A., and Ashwal, S. (2005). Proton MR spectroscopic imaging depicts diffuse axonal injury in children with traumatic brain injury. *AJNR Am. J. Neuroradiol.* 26, 1276–1285.
17. Babikian, T., Freier, M.C., Tong, K.A., Nickerson, J.P., Wall, C.J., Holshouser, B.A., Burley, T., Riggs, M.L., and Ashwal, S. (2005). Susceptibility weighted imaging: neuropsychologic outcome and pediatric head injury. *Pediatr. Neurol.* 33, 184–194.
18. Babikian, T., Alger, J.R., Ellis-Blied, M.U., Giza, C.C., Dennis, E., Olsen, A., Mink, R., Babbitt, C., Johnson, J., Thompson, P.M., and Asarnow, R.F. (2018). Whole brain magnetic resonance spectroscopic determinants of functional outcomes in pediatric moderate/severe traumatic brain injury. *J. Neurotrauma* 35, 1637–1645.
19. Govind, V., Gold, S., Kaliannan, K., Saigal, G., Falcone, S., Arheart, K.L., Harris, L., Jagid, J., and Maudsley, A.A. (2010). Whole-brain proton MR spectroscopic imaging of mild-to-moderate traumatic brain injury and correlation with neuropsychological deficits. *J. Neurotrauma* 27, 483–496.
20. Maudsley, A.A., Domenig, C., Govind, V., Darkazanli, A., Studholme, C., Arheart, K., and Bloomer, C. (2009). Mapping of brain metabolite distributions by volumetric proton MR spectroscopic imaging (MRSI). *Magn. Reson. Med.* 61, 548–559.
21. Malec, J.F., Brown, A.W., Leibson, C.L., Flaada, J.T., Mandrekar, J.N., Diehl, N.N., and Perkins, P.K. (2007). The Mayo Classification System for traumatic brain injury severity. *J. Neurotrauma* 24, 1417–1424.
22. Ghosh, N., Holshouser, B., Oyoyo, U., Barnes, S., Tong, K., and Ashwal, S. (2017). Combined diffusion tensor and magnetic resonance spectroscopic imaging methodology for automated regional brain analysis: application in a normal pediatric population. *Dev. Neurosci.* 39, 413–429.
23. Mohamed, M.A., Lentz, M.R., Lee, V., Halpern, E.F., Sacktor, N., Selnes, O., Barker, P.B., and Pomper, M.G. (2010). Factor analysis of proton MR spectroscopic imaging data in HIV infection: metabolite-derived factors help identify infection and dementia. *Radiology* 254, 577–586.
24. Dennis, E.L., Babikian, T., Alger, J., Rashid, F., Villalon-Reina, J.E., Jin, Y., Olsen, A., Mink, R., Babbitt, C., Johnson, J., Giza, C.C., Thompson, P.M., and Asarnow, R.F. (2018). Magnetic resonance spectroscopy of fiber tracts in children with traumatic brain injury: a combined MRS-diffusion MRI study. *Hum. Brain Mapp.* May 10. doi: 10.1002/hbm.24209. [Epub ahead of print]
25. Robertson, C.L., Scaffidi, S., McKenna, M.C., and Fiskum, G. (2009). Mitochondrial mechanisms of cell death and neuroprotection in pediatric ischemic and traumatic brain injury. *Exp. Neurol.* 218, 371–380.
26. Marmarou, A., Signoretti, S., Fatouros, P., Aygok, G.A., and Bullock, R. (2005). Mitochondrial injury measured by proton magnetic resonance spectroscopy in severe head trauma patients. *Acta Neurochir. Suppl.* 95, 149–151.
27. Signoretti, S., Vagnozzi, R., Tavazzi, B., and Lazzarino, G. (2010). Biochemical and neurochemical sequelae following mild traumatic brain injury: summary of experimental data and clinical implications. *Neurosurg. Focus* 29, E1.
28. Bigler, E.D., and Maxwell, W.L. (2011). Neuroimaging and neuropathology of TBI. *NeuroRehabilitation* 28, 63–74.
29. Wu, T.C., Wilde, E.A., Bigler, E.D., Li, X., Merkley, T.L., Yallampalli, R., McCauley, S.R., Schnelle, K.P., Vasquez, A.C., Chu, Z., Hanten, G., Hunter, J.V., and Levin, H.S. (2010). Longitudinal changes in the corpus callosum following pediatric traumatic brain injury. *Dev. Neurosci.* 32, 361–373.
30. Ommaya, A.K., and Gennarelli, T.A. (1974). Cerebral concussion and traumatic unconsciousness. Correlation of experimental and clinical observations of blunt head injuries. *Brain* 97, 633–654.
31. Adams, J.H., Doyle, D., Ford, I., Gennarelli, T.A., Graham, D.I., and McLellan, D.R. (1989). Diffuse axonal injury in head injury: definition, diagnosis and grading. *Histopathology* 15, 49–59.
32. Grados, M.A., Slomine, B.S., Gerring, J.P., Vasa, R., Bryan, N., and Denckla, M.B. (2001). Depth of lesion model in children and adolescents with moderate to severe traumatic brain injury: use of SPGR MRI to predict severity and outcome. *J. Neurol. Neurosurg. Psychiatry* 70, 350–358.
33. Babikian, T., and Asarnow, R. (2009). Neurocognitive outcomes and recovery after pediatric TBI: meta-analytic review of the literature. *Neuropsychology* 23, 283–296.
34. Catroppa, C., Anderson, V.A., Morse, S.A., Haritou, F., and Rosenfeld, J.V. (2007). Children's attentional skills 5 years post-TBI. *J. Pediatr. Psychol.* 32, 354–369.
35. Fay, G.C., Jaffe, K.M., Polissar, N.L., Liao, S., Rivara, J.B., and Martin, K.M. (1994). Outcome of pediatric traumatic brain injury at three years: a cohort study. *Arch. Phys. Med. Rehabil.* 75, 733–741.
36. Beck, L.H., Bransome, E.D., Jr., Mirsky, A.F., Rosvold, H.E., and Sarason, I. (1956). A continuous performance test of brain damage. *J. Consult. Psychol.* 20, 343–350.
37. Penfield, W., and Jasper, H.H. (1954). *Epilepsy and the Functional Anatomy of the Human Brain*. Little, Brown: Oxford, UK.
38. Van der Werf, Y.D., Jolles, J., Witter, M.P., and Uylings, H.B. (2003). Contributions of thalamic nuclei to declarative memory functioning. *Cortex* 39, 1047–1062.
39. Hall, E.D., Sullivan, P.G., Gibson, T.R., Pavel, K.M., Thompson, B.M., and Scheff, S.W. (2005). Spatial and temporal characteristics of neurodegeneration after controlled cortical impact in mice: more than a focal brain injury. *J. Neurotrauma* 22, 252–265.
40. Sherman, S.M., and Guillery, R. W. (2000). *Exploring the Thalamus*. Academic: New York.
41. Fearing, M.A., Bigler, E.D., Wilde, E.A., Johnson, J.L., Hunter, J.V., Xiaoyi, L., Hanten, G., and Levin, H.S. (2008). Morphometric MRI findings in the thalamus and brainstem in children after moderate to severe traumatic brain injury. *J. Child Neurol.* 23, 729–737.
42. Lutkenhoff, E.S., McArthur, D.L., Hua, X., Thompson, P.M., Vespa, P.M., and Monti, M.M. (2013). Thalamic atrophy in antero-medial and dorsal nuclei correlates with six-month outcome after severe brain injury. *Neuroimage Clin.* 3, 396–404.
43. Lifshitz, J., Kelley, B.J., and Povlishock, J.T. (2007). Perisomatic thalamic axotomy after diffuse traumatic brain injury is associated with atrophy rather than cell death. *J. Neuropathol. Exp. Neurol.* 66, 218–229.
44. Gooijers, J., Chalavi, S., Beeckmans, K., Michiels, K., Lafosse, C., Sunaert, S., and Swinnen, S.P. (2016). Subcortical volume loss in the thalamus, putamen, and pallidum, induced by traumatic brain injury, is associated with motor performance deficits. *Neurorehabil. Neural Repair* 30, 603–614.
45. De Simoni, S., Grover, P.J., Jenkins, P.O., Honeyfield, L., Quest, R.A., Ross, E., Scott, G., Wilson, M.H., Majewska, P., Waldman, A.D., Patel, M.C., and Sharp, D.J. (2016). Disconnection between the default mode network and medial temporal lobes in post-traumatic amnesia. *Brain* 139, Pt. 12, 3137–3150.
46. Giacino, J.T., Fins, J.J., Laureys, S., and Schiff, N.D. (2014). Disorders of consciousness after acquired brain injury: the state of the science. *Nat. Rev. Neurol.* 10, 99–114.
47. Scheibel, R.S. (2017). Functional magnetic resonance imaging of cognitive control following traumatic brain injury. *Front. Neurol.* 8, 352.
48. Gratton, C., Sun, H., and Petersen, S.E. (2017). Control networks and hubs. *Psychophysiology* 55. doi: 10.1111/psyp.13032. Epub 2017 Nov 28.
49. Posner, M.I., Rothbart, M.K., and Voelker, P. (2016). Developing brain networks of attention. *Curr. Opin. Pediatr.* 28, 720–724.
50. Mohan, A., Roberto, A.J., Mohan, A., Lorenzo, A., Jones, K., Carney, M.J., Liogier-Weyback, L., Hwang, S., and Lapidus, K.A. (2016). The Significance of the default mode network (DMN) in neurological and neuropsychiatric disorders: a review. *Yale J. Biol. Med.* 89, 49–57.
51. Ross, B.D., Ernst, T., Kreis, R., Haseler, L.J., Bayer, S., Danielsen, E., Bluml, S., Shonk, T., Mandigo, J.C., Caton, W., Clark, C., Jensen, S.W., Lehman, N.L., Arcinieg, E., Puden, R., and Shelden, C.H. (1998). 1H MRS in acute traumatic brain injury. *J. Magn. Reson. Imaging* 8, 829–840.
52. Maudsley, A.A., Govind, V., Saigal, G., Gold, S.G., Harris, L., and Sheriff, S. (2017). Longitudinal MR spectroscopy shows altered metabolism in traumatic brain injury. *J. Neuroimaging* 27, 562–569.

Address correspondence to:  
 Barbara Holshouser, PhD  
 Department of Radiology  
 Loma Linda University Health  
 CSP Room C1025  
 11175 Campus Street  
 Loma Linda, CA 92354

E-mail: bholshouser@llu.edu